

Wide Angle Astrometry

Don Hutter

August 11, 1999

Outline:

- Motivation (10 minutes)
 - scientific goals (optical)
 - scientific goals (infrared)
- Observables and astrometric solution (10 minutes)
 - basic quantities required for astrometric sol'n
 - outline of astrometric solution
- Practical implementation (15 minutes)
 - delay measurement and dispersion compensation
 - baseline metrology
 - 'constant' term measurement
- Summary (5 minutes)
 - present status and prospects

Motivation:

Why attempt wide-angle astrometry from ground?

* Optical:

- Hipparcos positional accuracies will degrade to ~ 10 mas by 2001 due to proper motion uncertainties.

- NPOI Goal:

Catalog of ~ 1000 stars, 1-3 mas

- * longer timebase to improve proper motions
(Also separate binary/proper motions)

- * observations (both astrometric and imaging) of radio stars to tie to ICRS

\Rightarrow relative rotation of b/w Hipparcos and ICRS
(currently ~ 0.25 mas/yr)

\Rightarrow zonal errors in Hipparcos catalog?

Infrared:

IR (1.25-2.2 μm) fringe detection under development at NPOI:

- Mira Variables:
 - Want accurate parallaxes to get linear radii. These lead to choice b/w fundamental or first-overtone pulsation. This leads to P-L-M relationship.
 - Because Miras are very luminous, they may be used as distance indicators (for example to the LMC).
 - Hipparcos not rich in well determined Mira parallaxes.

- Embedded Sources:

- young stars buried in molecular clouds
- bright at IR and radio wavelengths
- no (or very faint) optical counterparts

Examples: BN source in Orion, S140 IRS 1, S106 IR

- * Want accurate positions to compare to radio positions, particularly for BN, where other IR and radio sources are measured to assumed position of BN at each wavelength.
- * Best IR position for BN $\pm 0.''1$.
Best radio position of BN counterpart $\pm 0.''03$.
- * Also want proper motions to determine whether BN is just a runaway star. Radio position associated with BN appears to be moving at 20 mas/yr.

- Evolved stars with dense circumstellar shells:
 - bright in IR
 - faint optical counterpart
- * Examples: NML Cyg, IRC +10216
- * Want to compare optical and radio positions.
 - best determined position for NML Cyg is $\pm 0.''03$
 - improved position to allow alignment wrt to masers

Basic Quantities:

* Delay:

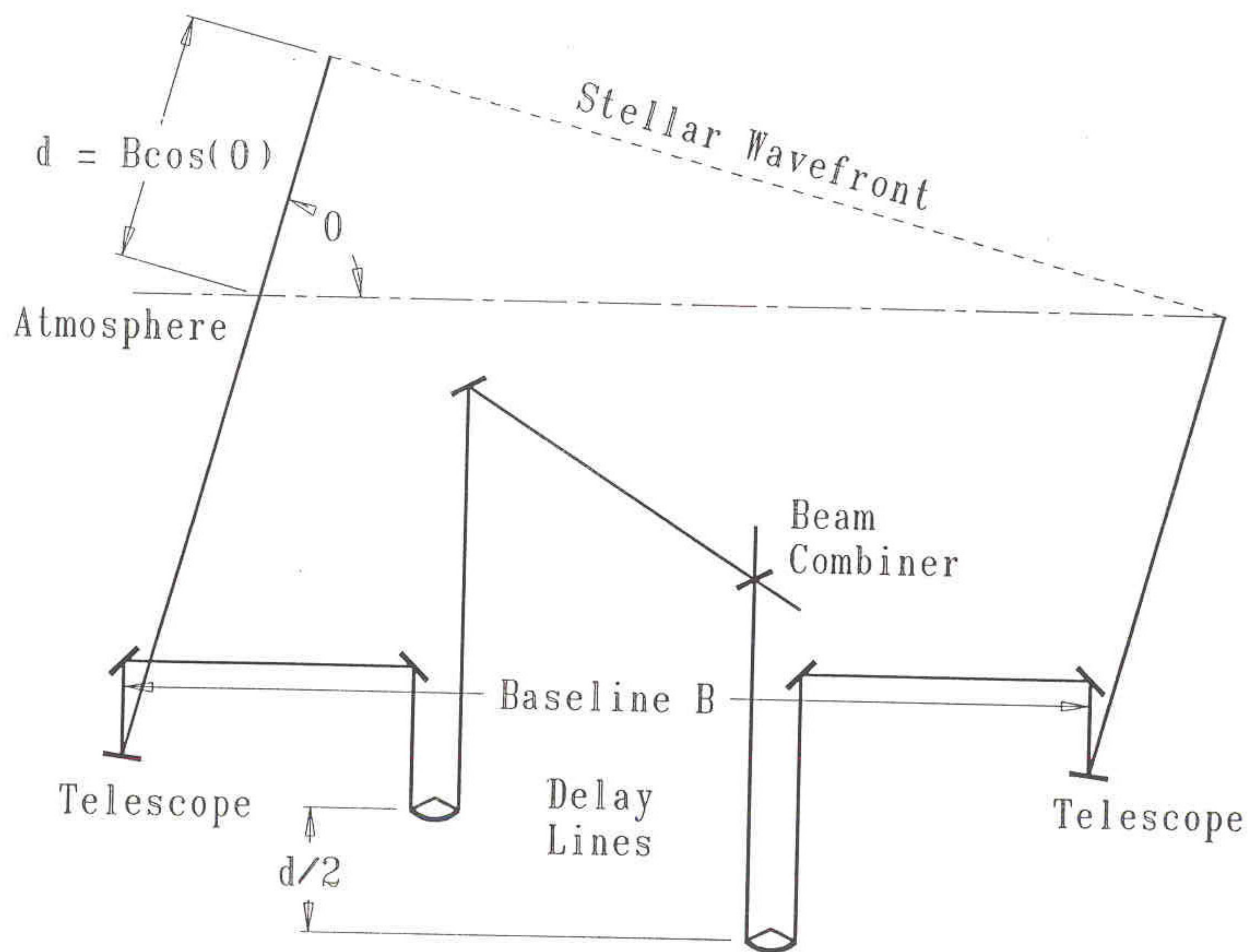
- difference in delay line positions as measured by laser metrology
- measurement in vacuum \Rightarrow atmospheric refraction does not effect measured delays

* Baseline

- can use any point on mirror surfaces

* 'Constant-term'

- OPL difference b/w light paths



Schematic Layout of a Michelson Interferometer

Hines et al 1990 (SPIE)

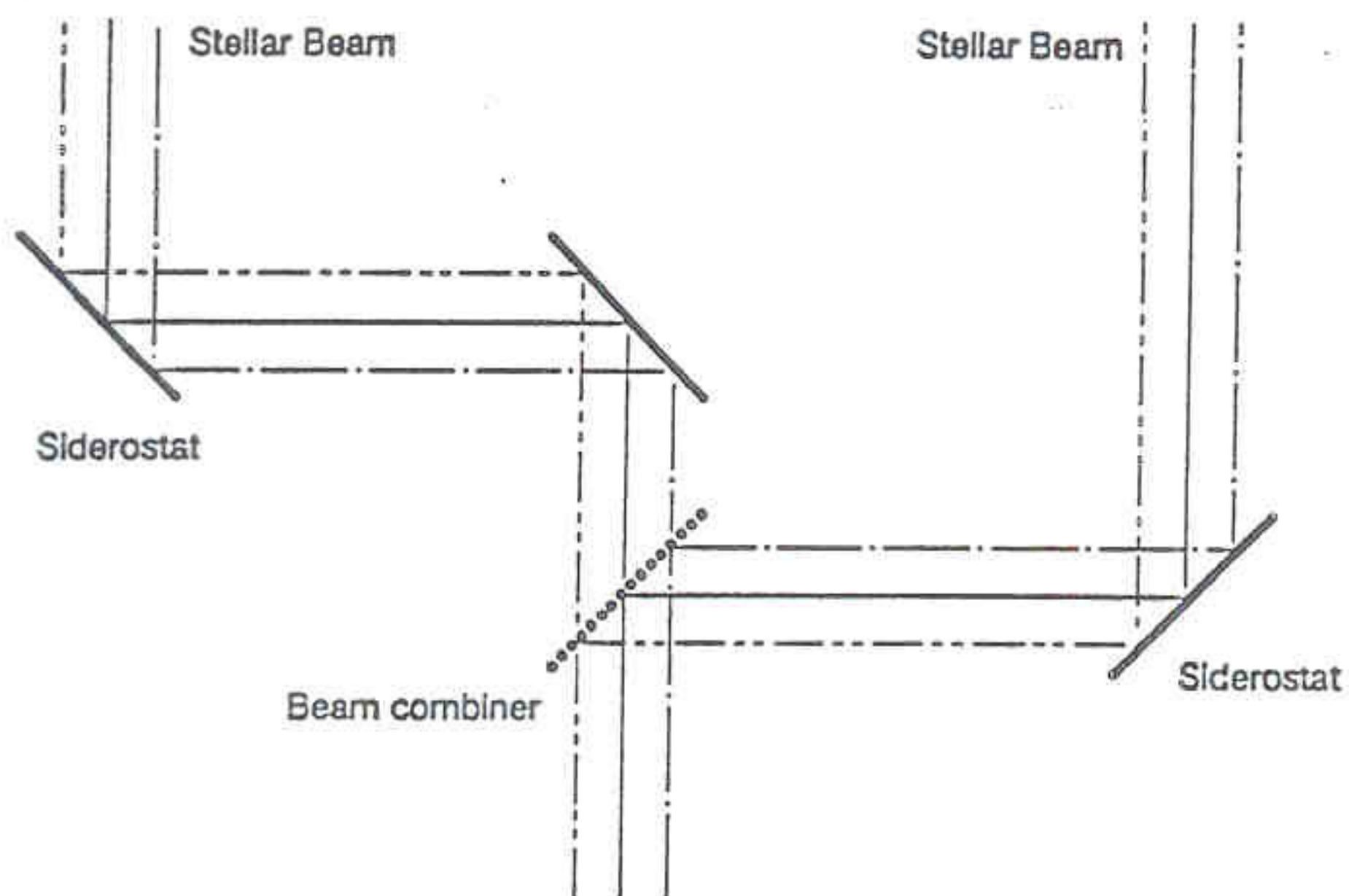


Figure 7. Pseudo-pivot lemma. Any point on the surface of the mirror can be used as the end of the baseline.

Astrometric Solution:

- For a single baseline (*e.g.*, Hummel *et al.* 1994):

$$d_G(t) = \mathbf{B}(t) \cdot \mathbf{s}_0 + C,$$

where:	$d_G(t)$	=	geometrical delay
	$\mathbf{B}(t)$	=	baseline vector
	\mathbf{s}_0	=	star position unit vector
	C	=	'constant' term

- Since the baseline coordinates cannot be known *a priori* with sufficient accuracy, must solve for these simultaneously with star positions:

$$d_G(t) = C_0 + B_z \sin \delta - B_y \cos \delta \sinh(t) + B_x \cos \delta \cosh(t),$$

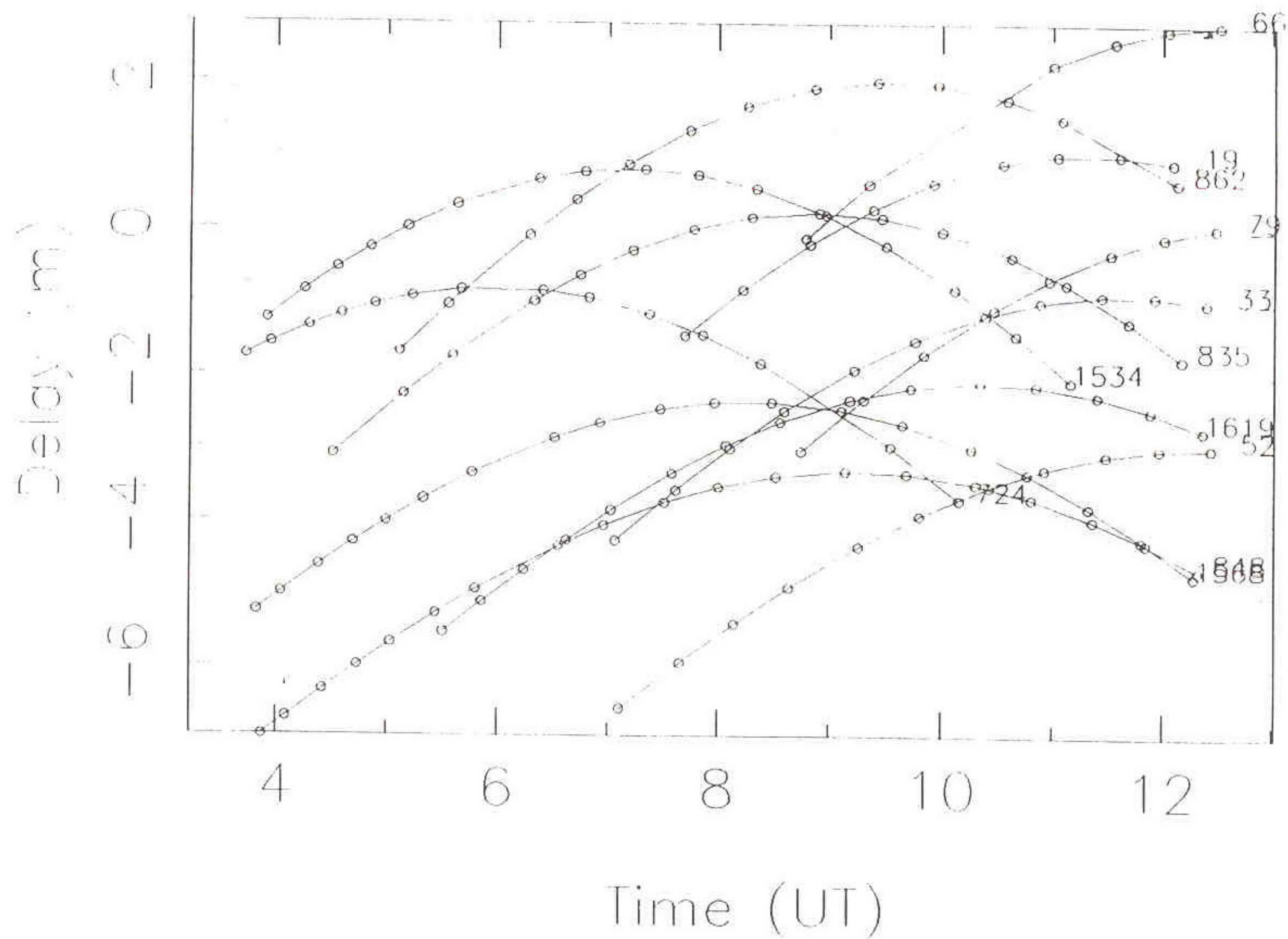
where	$h(t)$	=	hour angle at sidereal time t
	δ	=	declination of star

- In terms of assumed baseline components and star positions, plus small offsets:

$$\begin{aligned} d_{\text{res}}(t) &= d(t, \delta + \Delta\delta, \alpha + \Delta\alpha, \mathbf{B} + \Delta\mathbf{B}) - d(t, \delta, \alpha, \mathbf{B}) \\ &= X \cosh(t) - Y \sinh(t) + Z, \end{aligned}$$

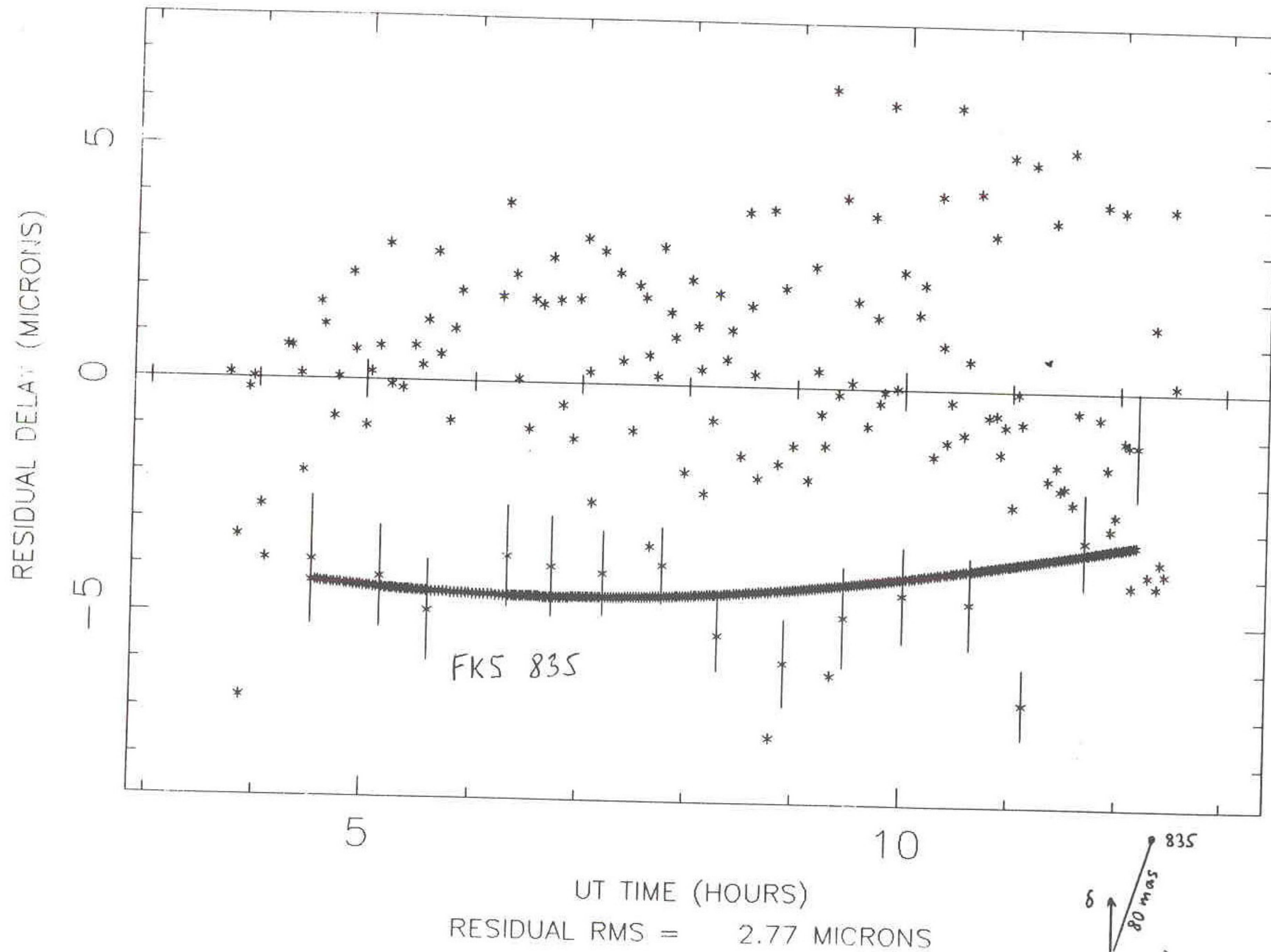
where:	X	$= \Delta B_x \cos \delta - \Delta \delta B_x \sin \delta + \Delta \alpha B_y \cos \delta$
	Y	$= \Delta B_y \cos \delta - \Delta \delta B_y \sin \delta - \Delta \alpha B_x \cos \delta$
	Z	$= \Delta B_z \sin \delta + \Delta \delta B_z \cos \delta + C_0$

Delays on 920808



8 AUG 1992

N-S CONSTANT BASELINE



Measure d_{res} for each star over range of hour angles $\Rightarrow X, Y, Z$

IF observe ≥ 3 stars \Rightarrow solve for all unknowns simultaneously

BUT, B_x, B_y, B_z and C all vary on time scales as short as a SINGLE observation!

- thermal drifts (10's of $\mu\text{m}/\text{hour}$)
- mechanical imperfections in siderostats
($\sim 10 \mu\text{m}$ motion of siderostat b/w stars)
- atmosphere also induces large, rapid ($\sim 30 \mu\text{m}$) delay fluctuations!

Dispersion Compensation:

- For Mark III (phase tracking interferometer):
 - track white light central fringe in wide (300nm) channel, while use delays in narrow channels ($\sim 25\text{-}40\text{nm}$) at 500nm, 550nm, and 800nm to derive vacuum delays (ref: Colavita *et al.* 1987).
 - estimate vacuum delay by the “two-color” delay d_{2C} ,

$$d_{2C} \equiv d_{\text{red}} - D(d_{\text{blue}} - d_{\text{red}}), \text{ where}$$

$$D = (n_{\text{red}} - 1)/(n_{\text{blue}} - n_{\text{red}})$$

= dispersion constant (constant for dry air)

$$\approx 100 (550\text{nm}/800\text{nm}), \approx 71 (500\text{nm}/800\text{nm})$$

- two-color corrected delays show reduced low-frequency variations relative to the one-color delay in wide tracking channel.
- however, small bandwidth in two-color channels result in higher photon noise which in practice limited uncertainty of two-color delay measurements to $\sim 2 \mu\text{m}$.

328 HUMMEL *ET AL.*: ASTROMETRIC MEASUREMENTS

328

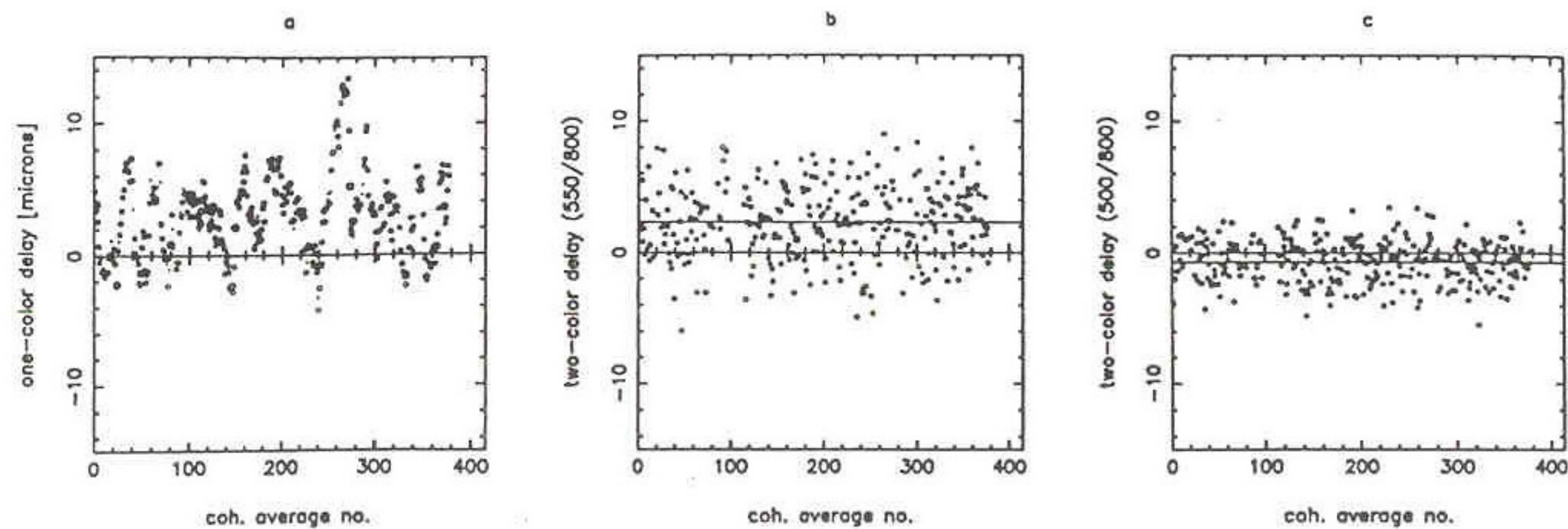


FIG. 2. Measurements of the one-color delay in the tracking channel (a) and two-color delays (b), (c) in a scan of 75 s duration. Data points are 200 ms coherent averages.

Delay Measurement: (NPOI)

* Group delay fringe tracking:

- fringes dispersed over 32 spectral channels
- modulate each baseline a few λ
- synchronously count photons in 8 bins for 2 ms
- complex FT for each spectral channel \Rightarrow complex fringe visibility
- 2nd FT over 32 channels \Rightarrow group delay error signal

* Coherent averaging:

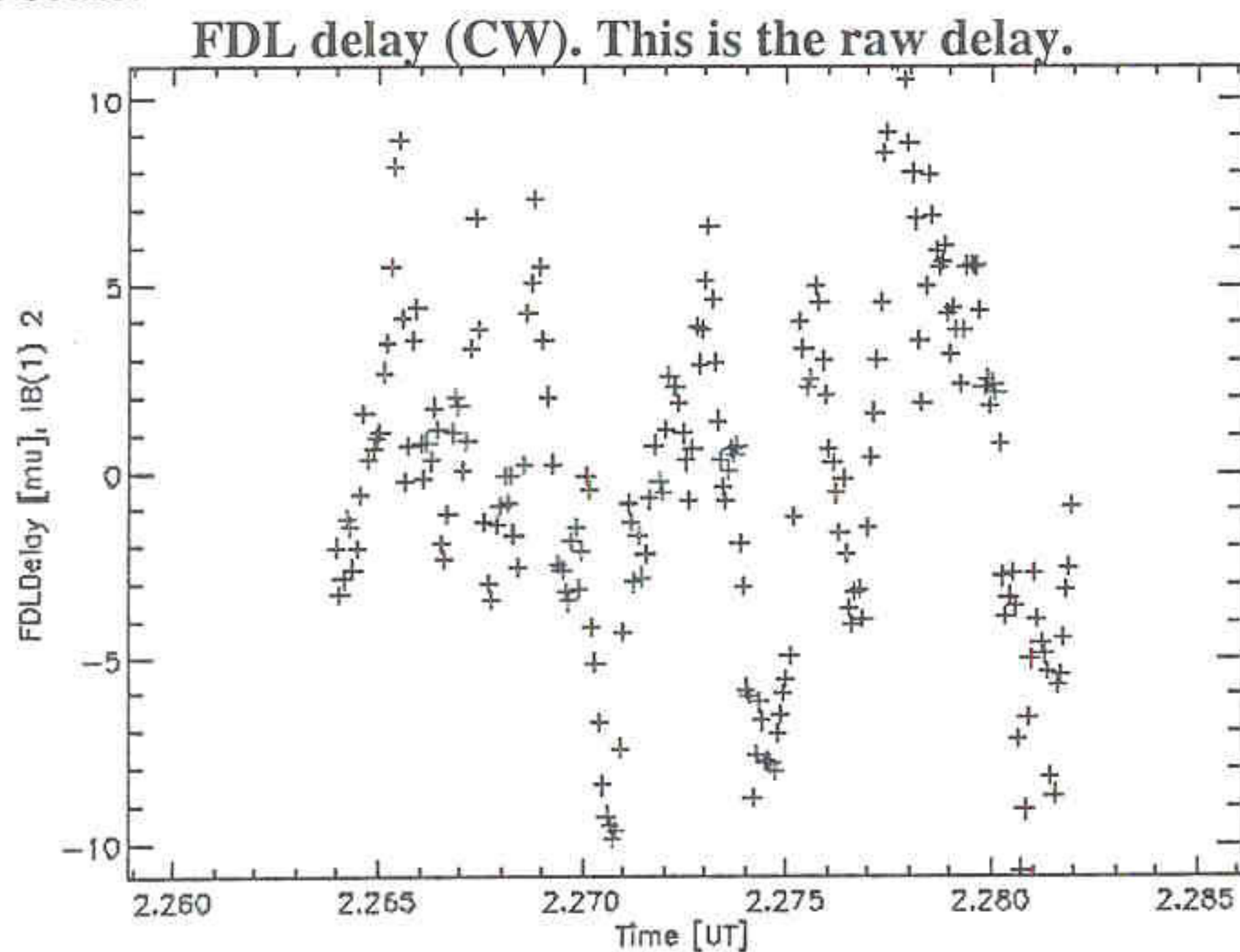
- Knowledge of group delay for each 2 ms allows one to rotate the complex visibility phasors by $e^{(2\pi i d \sigma)}$, where d = group delay & σ = wave number of spectral channel.
- This allows coherent addition of the data to provide sufficient SNR to allow dispersion correction:

Atmospheric Dispersion Compensation:

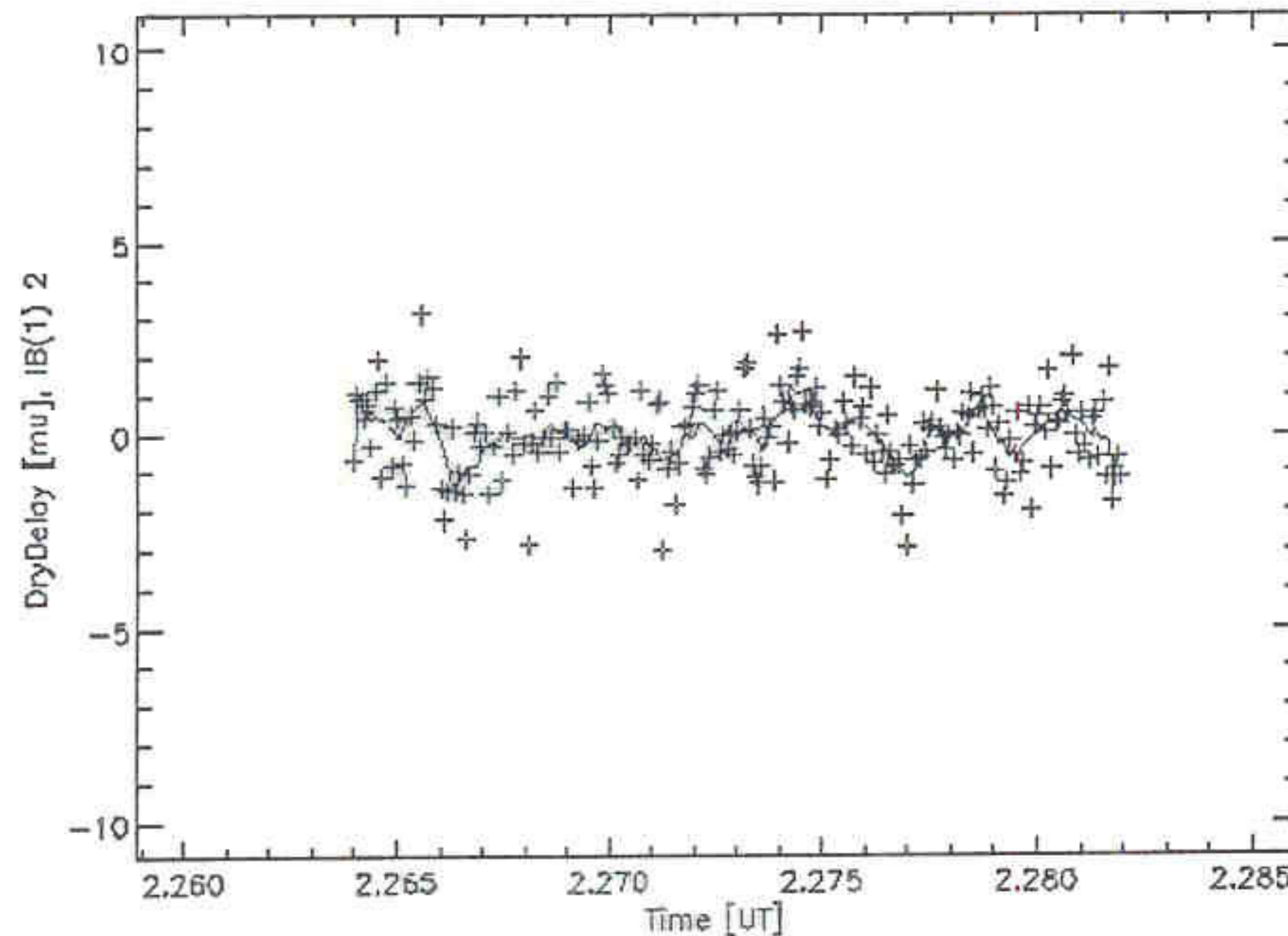
- On each baseline, the variation of the observed fringe phase with wave number (spectral channel), $\phi_A(\sigma)$ can be used to estimate the OPL change (air path mismatch b/w stations) due to the atmosphere, because $n(\sigma)-1$ has a significant σ^2 dependence at optical wavelengths.
- Can express as $\phi_A(\sigma) = \phi_A(\sigma_0)[D_1 + \sigma D_2 + \Phi(\sigma)]$, where the $\Phi(\sigma)$ term makes it possible to determine the air path mismatch and hence correct the observed delay to the geometrical delay value (first term is constant phase offset, second term is indistinguishable from star position offset).

NPOI dispersion correction

Here is a little bit of information on how much we improve the delay measurements by applying dispersion corrections. These results are for a 60s scan on FKV0201, on 1998-02-13, CW. Each individual integration is 200ms of data. The following plots have the same scale.



DRY delay (CW). This is the (dry air) dispersion corrected delay. A line (9-pt averages) indicates the remaining systematic variations.



The reduction in RMS achieved by dispersion corrections is at least a factor of about 5. Longer integration results in a smaller RMS, but levels out at 0.45 microns between 1s and 2s. Here the reduction is 8-fold over the non-white FDL delay variations.

Reducing the RMS [microns] through integration

Number of samples in average	RMS (DryDelay)	RMS (FDLDelay)
1	1.02	4.7
3	0.72	
5	0.61	
7	0.55	
9	0.51	4.0
11	0.48	
13	0.46	
15	0.45	
17	0.45	3.6

Status:

- While dispersion correction sometimes produces up to 5 x reduction in the rms of the coherently averaged data, the current technique breaks down for any but the brightest (~2nd magn.) sources.
 - particularly vexing, since dispersion correction worked poorly on (relatively faint, red) internal light source used in constant-term measurements.
- Developing a technique that uses the fact that the group-delay corrected visibility phasors should vary in a relatively continuous and slow way to smooth the data before computing the mean, dispersion-corrected delays.

Baseline Metrology:

- 100 nm baseline metrology system necessary for 1 mas astrometry on 20 m baseline.
 - NPOI: 55 monitored paths
 - tie baseline to local bedrock \Rightarrow absolute declinations
- Subsystems:
 - reference table to siderostat metrology
 - optical anchors
 - pier to pier

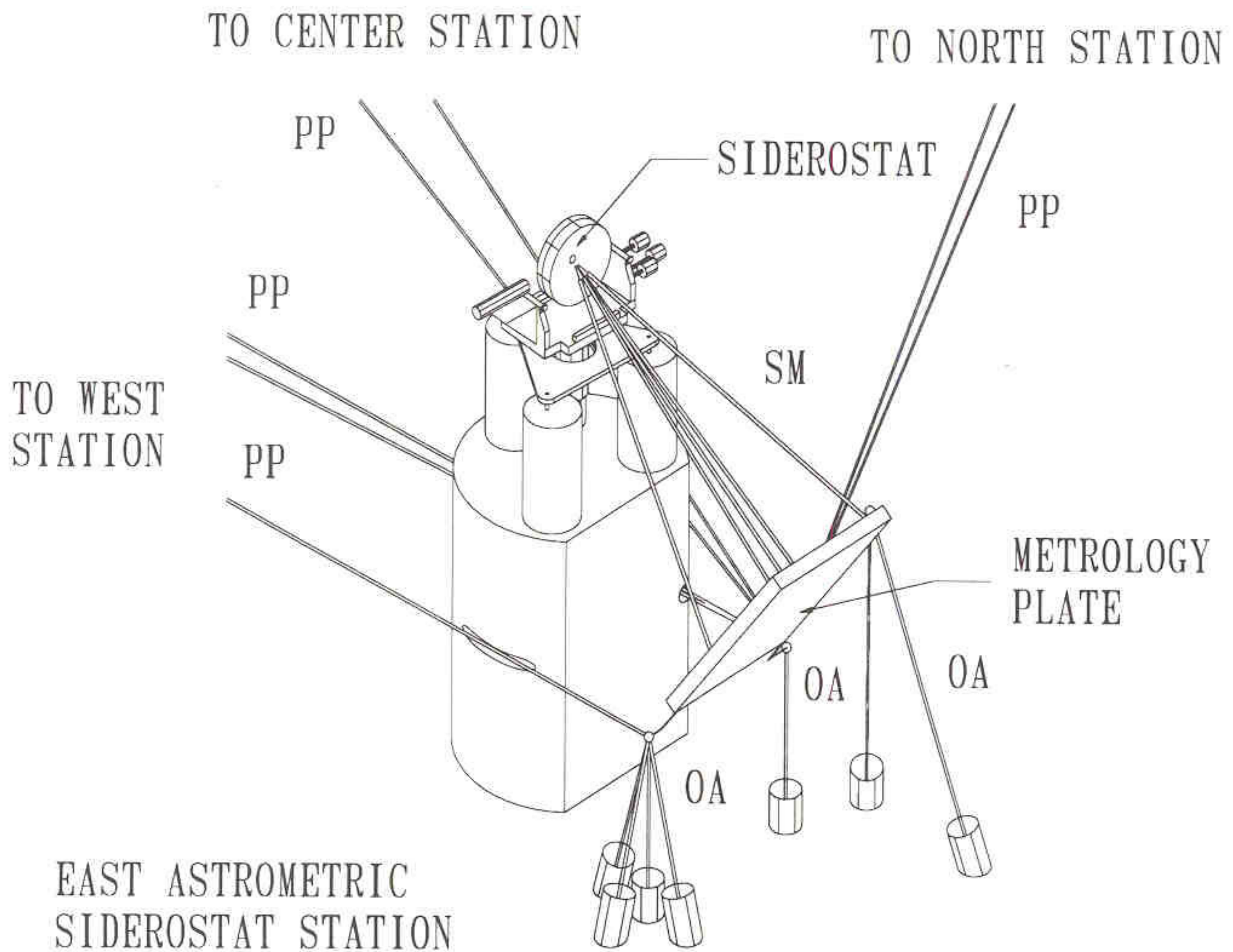
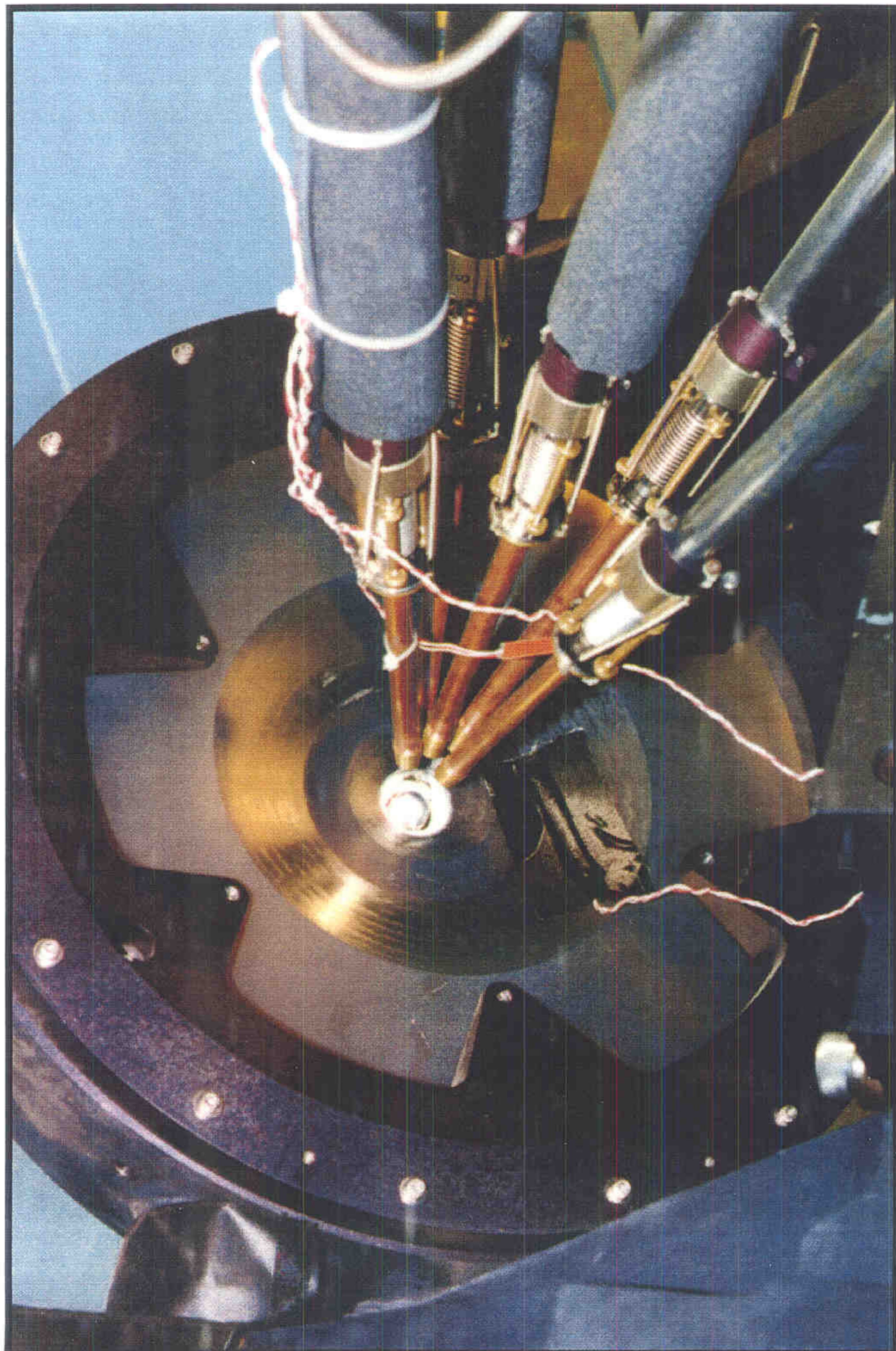
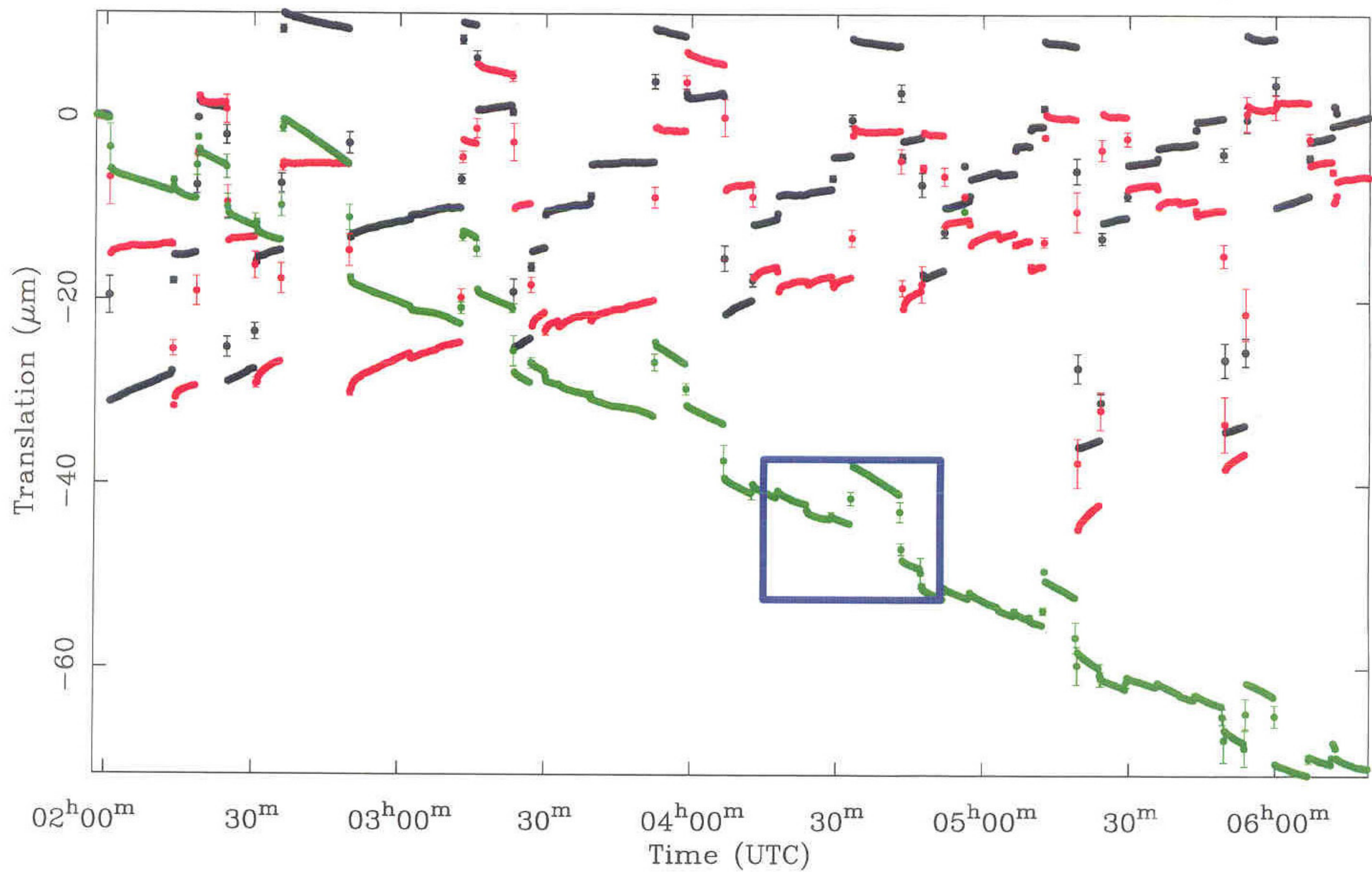
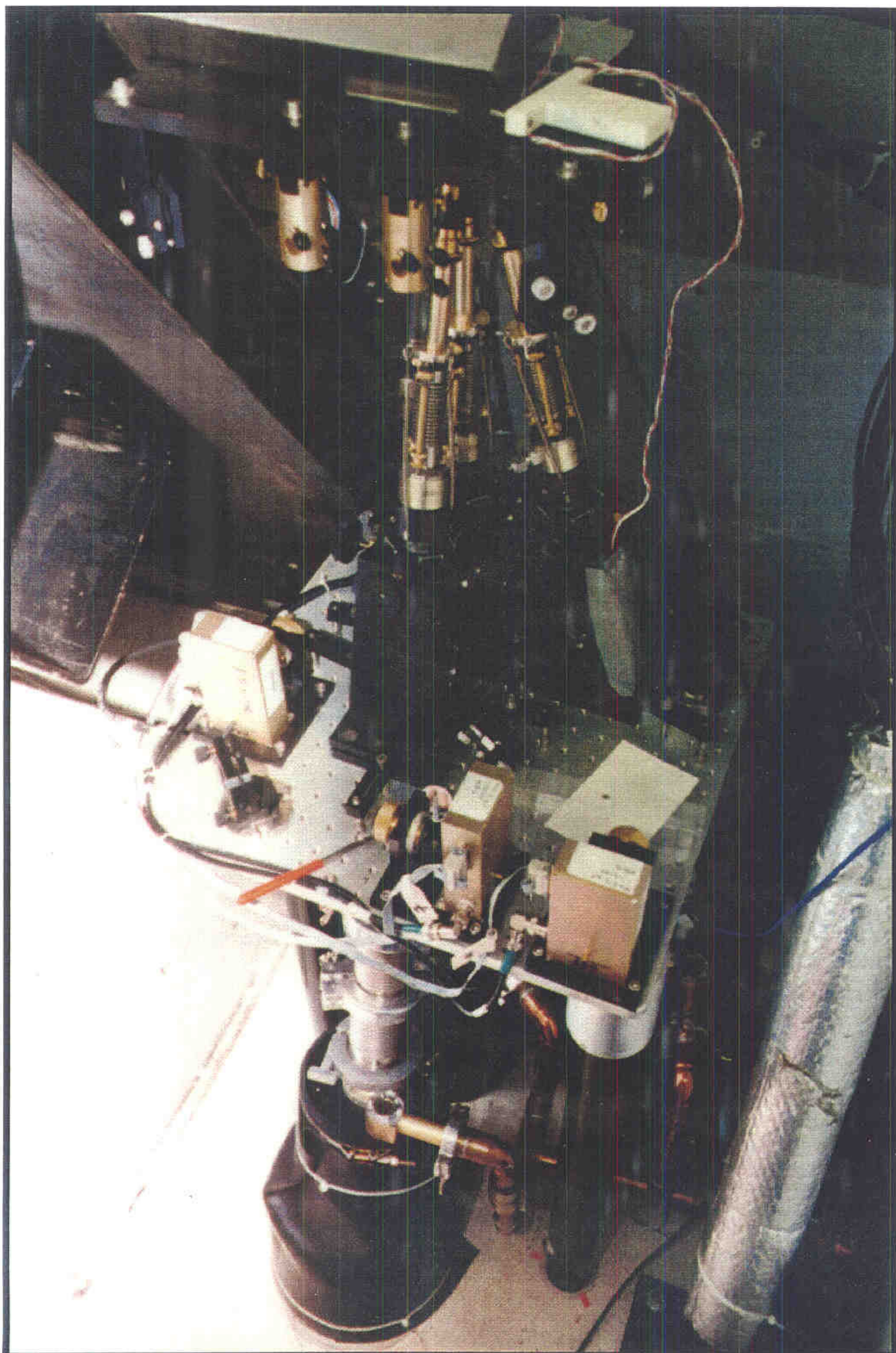


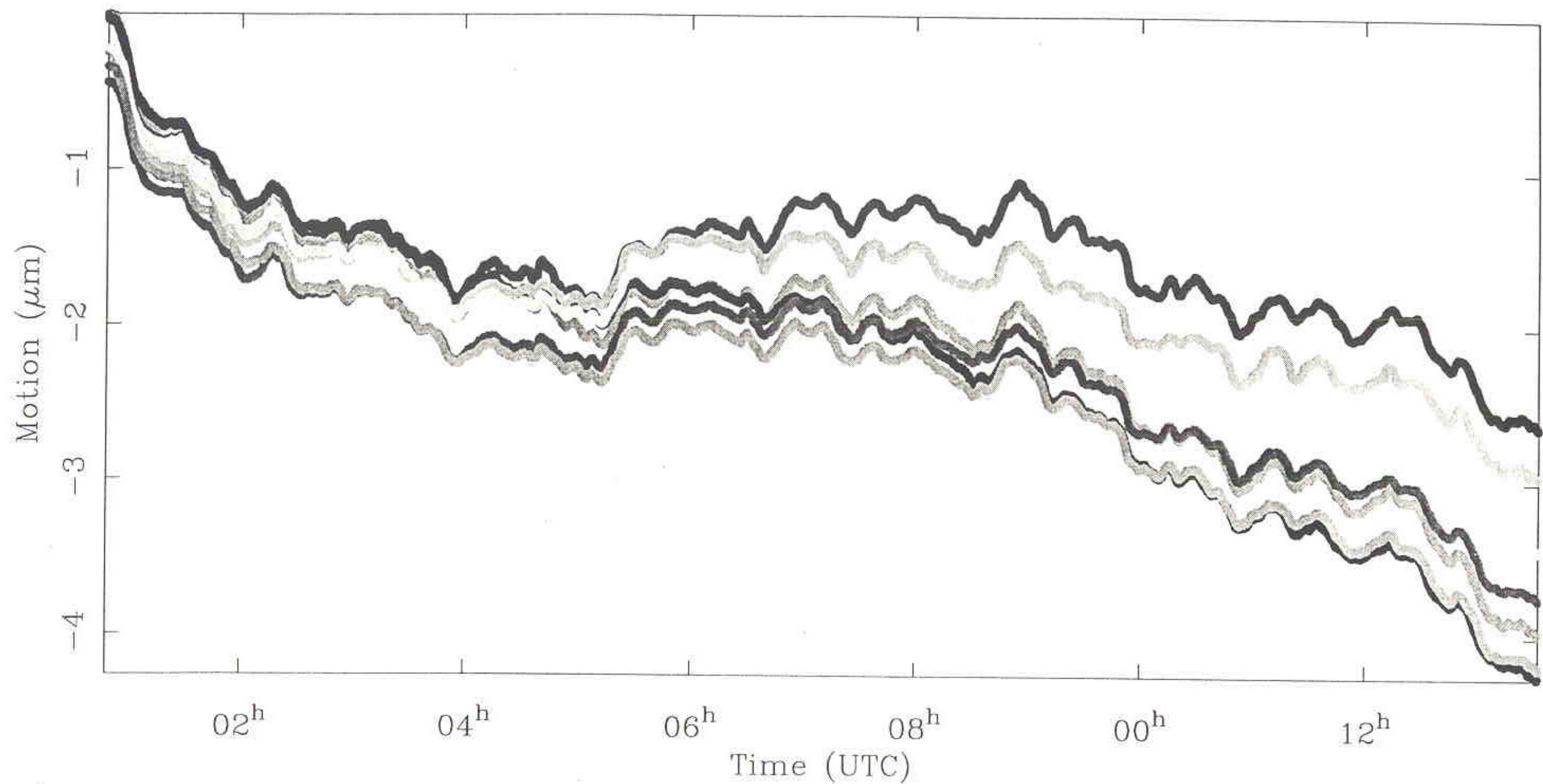
Figure 6. The baseline metrology system of the NPOI consists of 60 laser interferometers configured (in three subsystems) to monitor changes in the locations of the siderostats, in three dimensions, with respect to the local bedrock. This elevation view of the east astrometric siderostat station shows parts of the three metrology subsystems: the siderostat metrology (SM; five beams), which monitors the distance from the metrology plate to the siderostat pivot point; the optical anchor metrology (OA; seven beams), which monitors the motion of the metrology plate with respect to bedrock 7 m below the surface; and the pier-to-pier metrology (PP; seven beams), which monitors the horizontal motions of the metrology plates with respect to one another.





Translation (μm), sid 1 disp t1
 Translation (μm), sid 1 disp t2
 Translation (μm), sid 1 disp t3





Motion (μm), oa 2 1 1 (I/F Box = 1, Channel = 7)

Motion (μm), oa 2 1 2 (I/F Box = 1, Channel = 8)

Motion (μm), oa 2 2 1 (I/F Box = 1, Channel = 6)

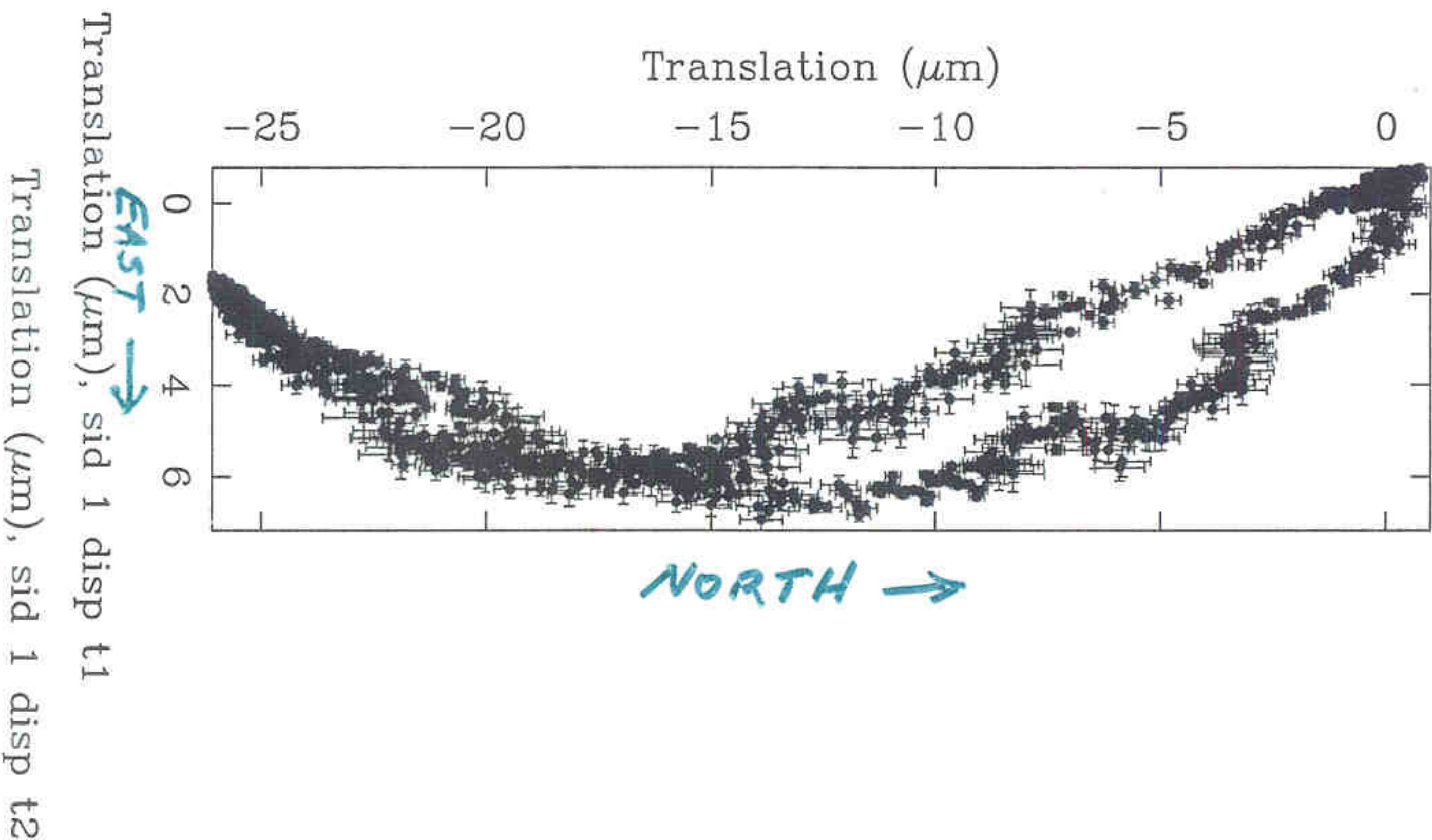
Motion (μm), oa 2 3 1 (I/F Box = 2, Channel = 1)

Motion (μm), oa 2 3 2 (I/F Box = 2, Channel = 2)

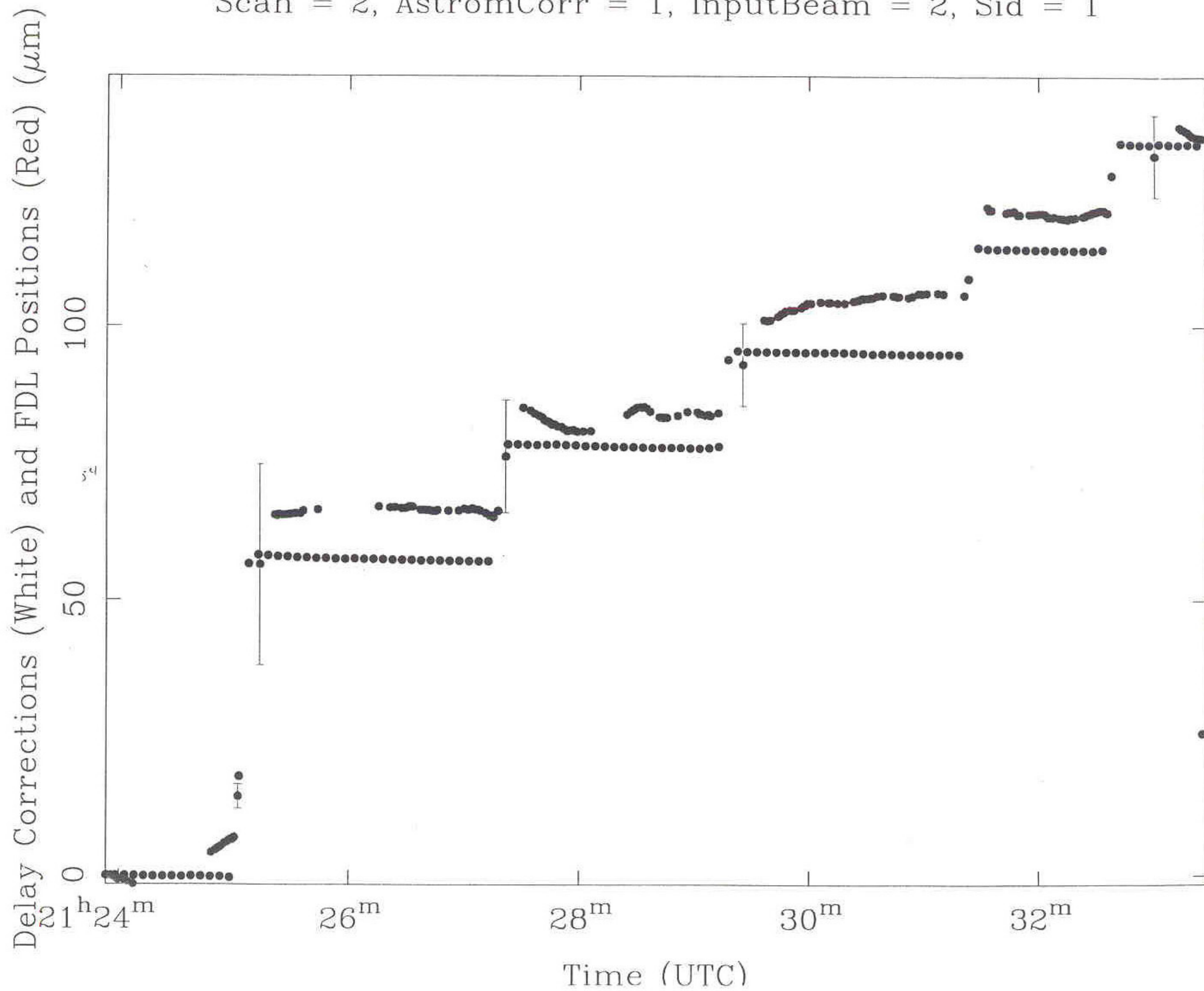
Motion (μm), oa 2 3 4 (I/F Box = 2, Channel = 4)

Status:

- Repeatability measurements to 200 nm
- Baseline metrology repeatably reproduces known, instantaneous translations of siderostat pivots in 3-D at level of $\sim 1 \mu\text{m}$ rms (= level of accuracy in applying translations).
- Resulting (instantaneous) changes in white light fringe delays match those observed to $\sim 1 \mu\text{m}$ as well.
- However, observed delays exhibit large longer-term drifts, both while observing stars and internal source, that are not predicted from baseline metrology data:
 - due apparently to poor dispersion correction on fainter sources, and unmeasured/uncompensated C-term drifts



Scan = 2, AstromCorr = 1, InputBeam = 2, Sid = 1



Constant Term:

- Alternative measurement techniques:
 - 1) for slow, smooth variations in internal path lengths
 - ⇒ periodically fringe track internal source with siderostats in autocollimation
 - practical limit: every 30 min
 - interpolate values to time of stellar observations
 - add additional correction due to instantaneous siderostat pivot position (from baseline metrology)
 - 2) rapid and/or discontinuous internal path variations:
 - ⇒ single-color (relative) internal path metrology to interpolate b/w autocoll. observations, or:
 - ⇒ two-color (absolute) metrology

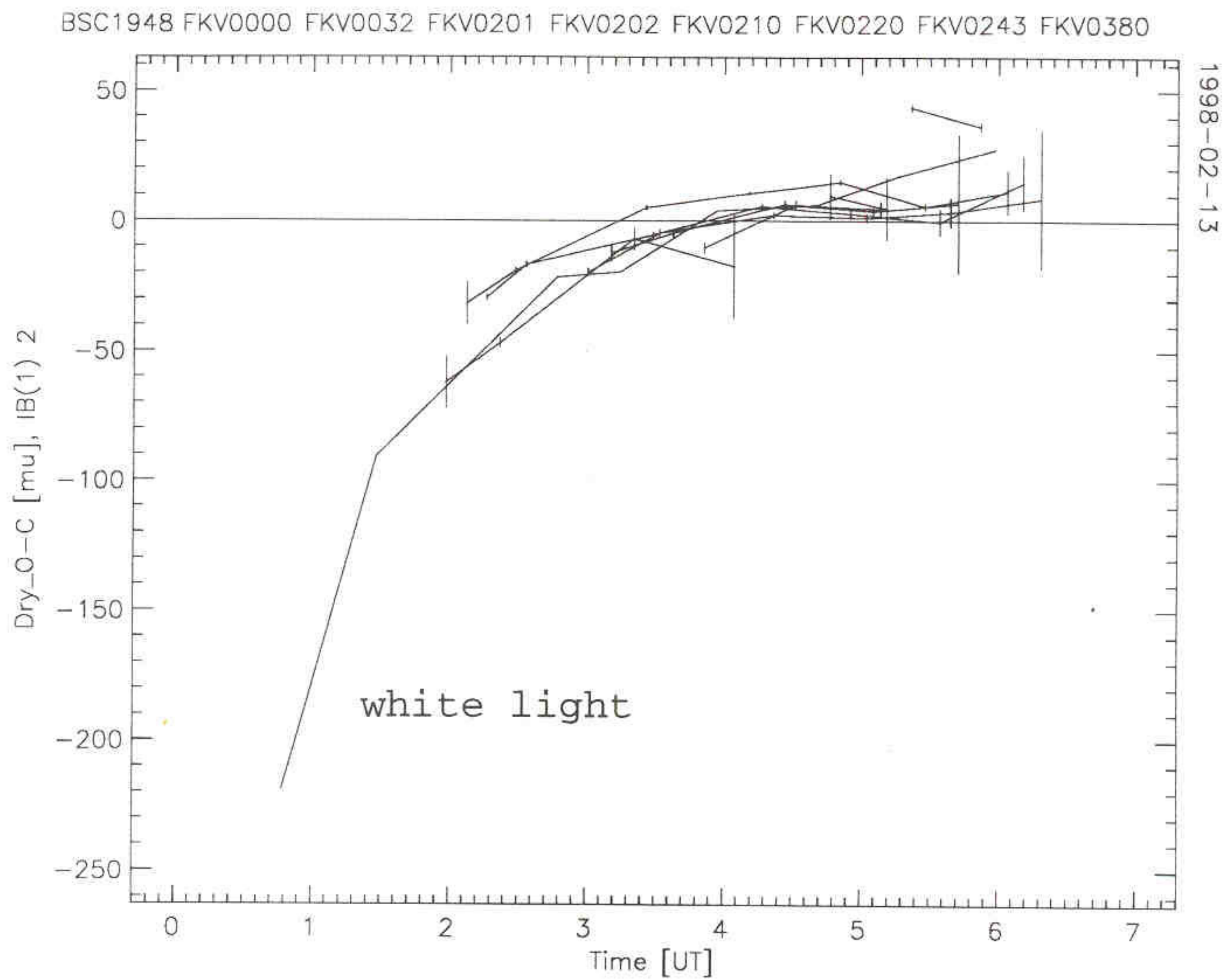


Figure 4. The data from Fig. 3 with the observed white light fringe measurements superimposed.

$N=36$ $\sigma=7.81$

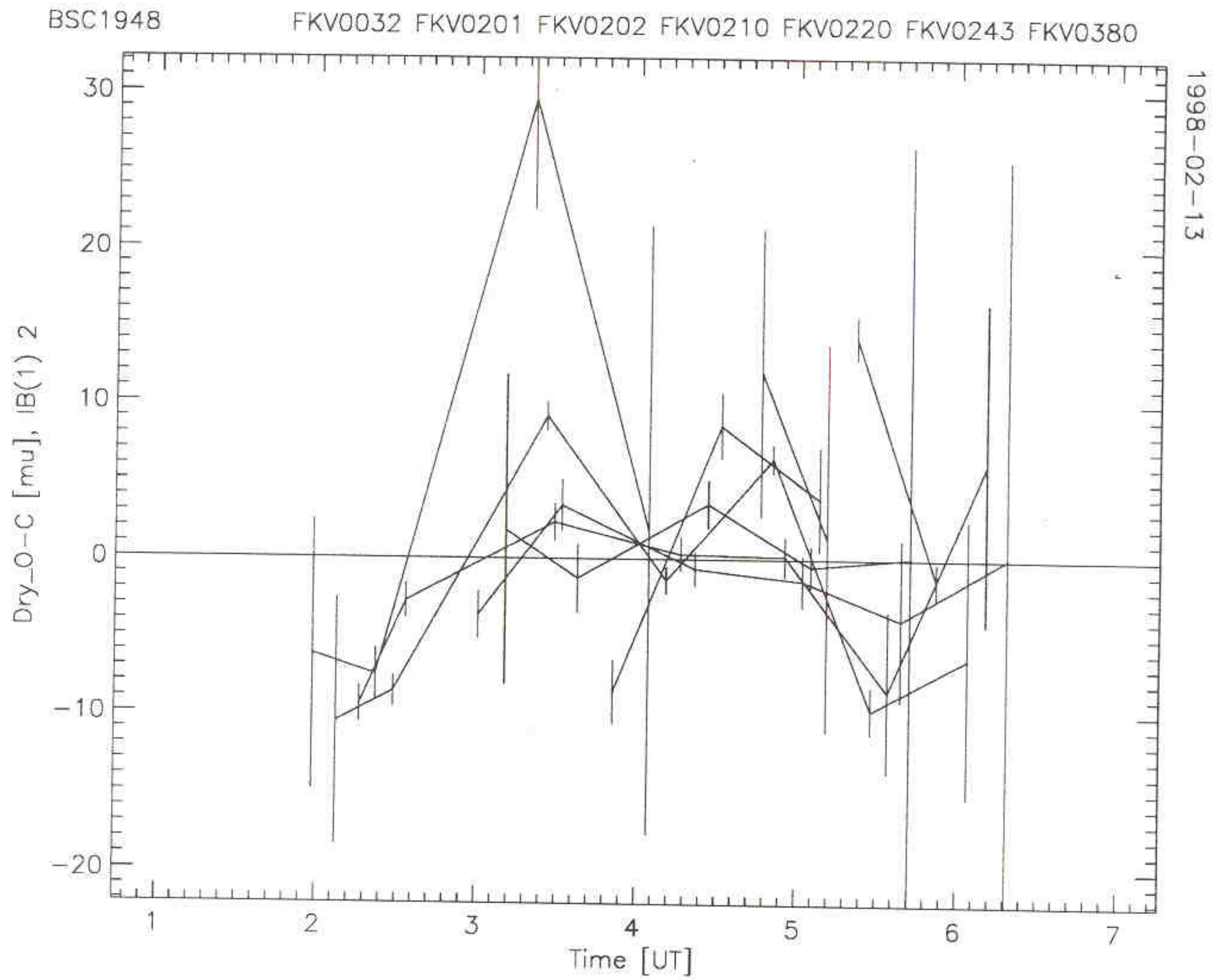
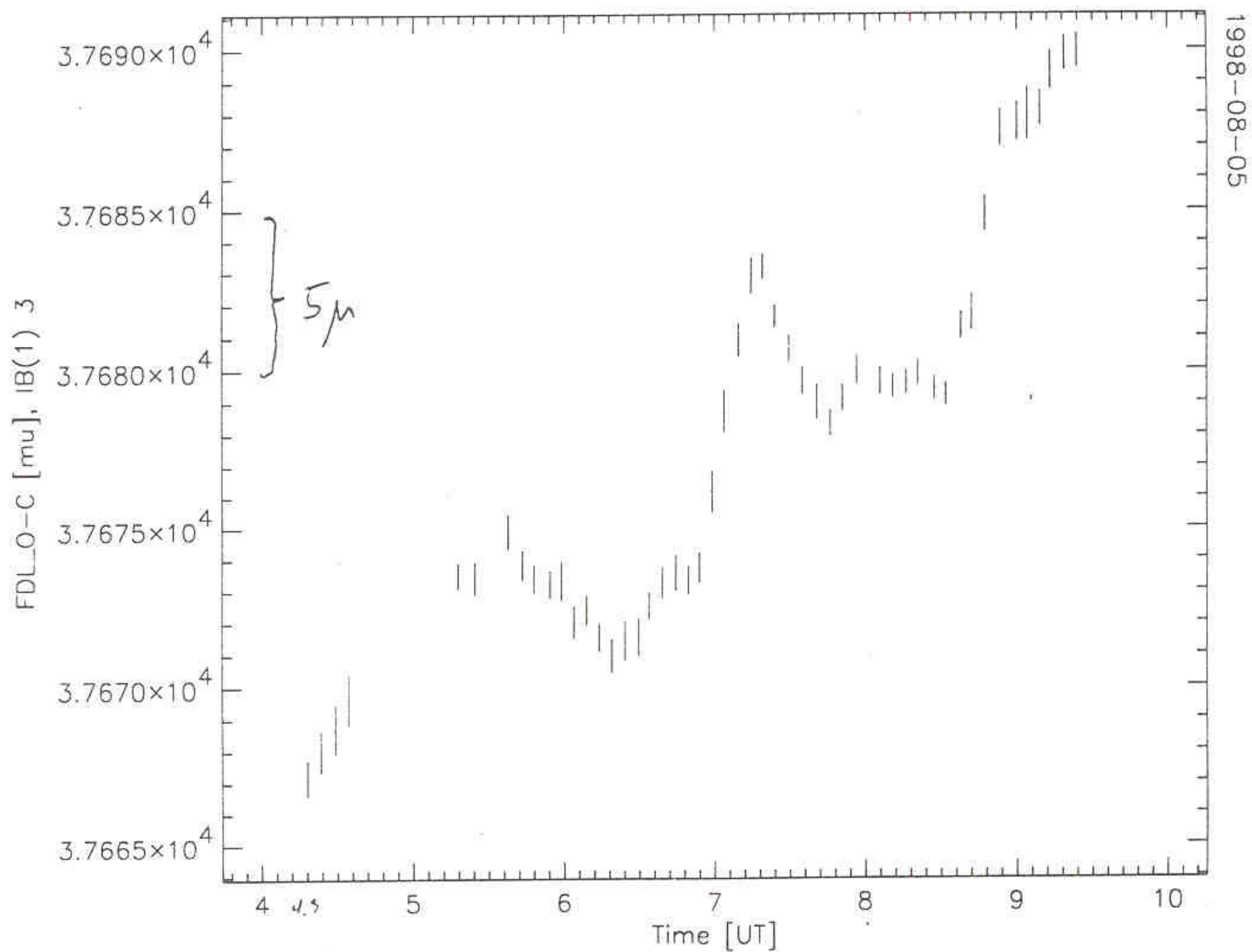


Figure 5. Data from Fig. 3, after correction for the white light fringe measurements. Note the lack of obvious long-term trends in the residuals from the (again refitted) baseline.

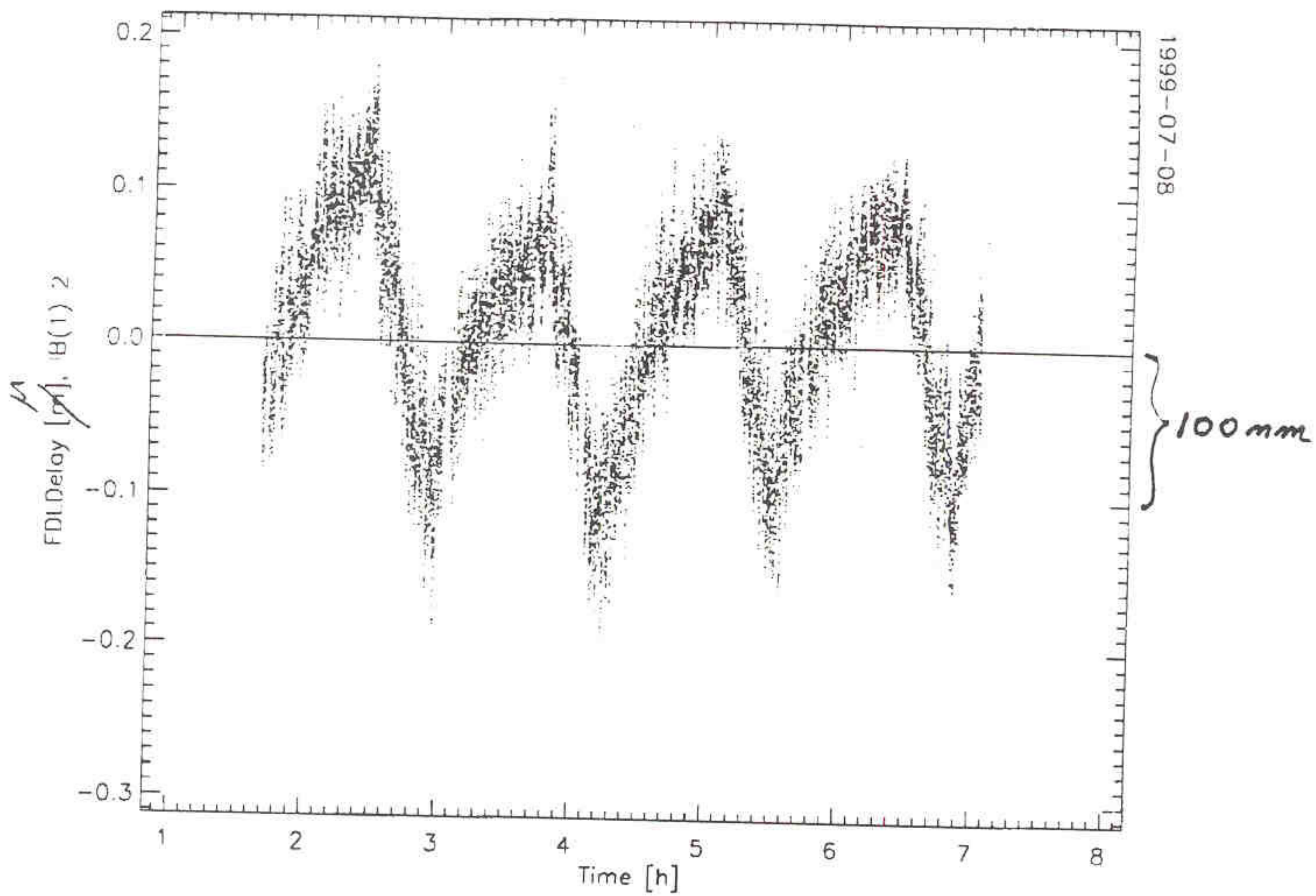
Status:

- Lengthy autoll. observations initially show internal path drifts of up to $40\text{ }\mu\text{m/hour}$ \Rightarrow poor correction!
 - measured siderostat pivot motion only contributes $\sim 10\%$
- Simple insulation of feed system vacuum cans reduces long-term drifts to as low as $\sim 1\text{ }\mu\text{m/hour}$, but with $\pm 5\text{ }\mu\text{m}$ oscillations.
 - $\Rightarrow 1\text{-}2\text{ }\mu\text{m}$ measurement errors w/30 min sampling
- But, autocoll. Observations within beam combining room, where temperatures are routinely stabilized to $< 0.1\text{C}$ show sub-micron path stability.
 - $\Rightarrow \leq 1\text{ }\mu\text{m}$ path stability may be possible with good mechanical/thermal control of feed system components.
 - currently, upgrading feed components and adding internal temperature sensors.
 - conducting autocoll. tests from various points in feed system to locate sources of path instability.

FKV0000

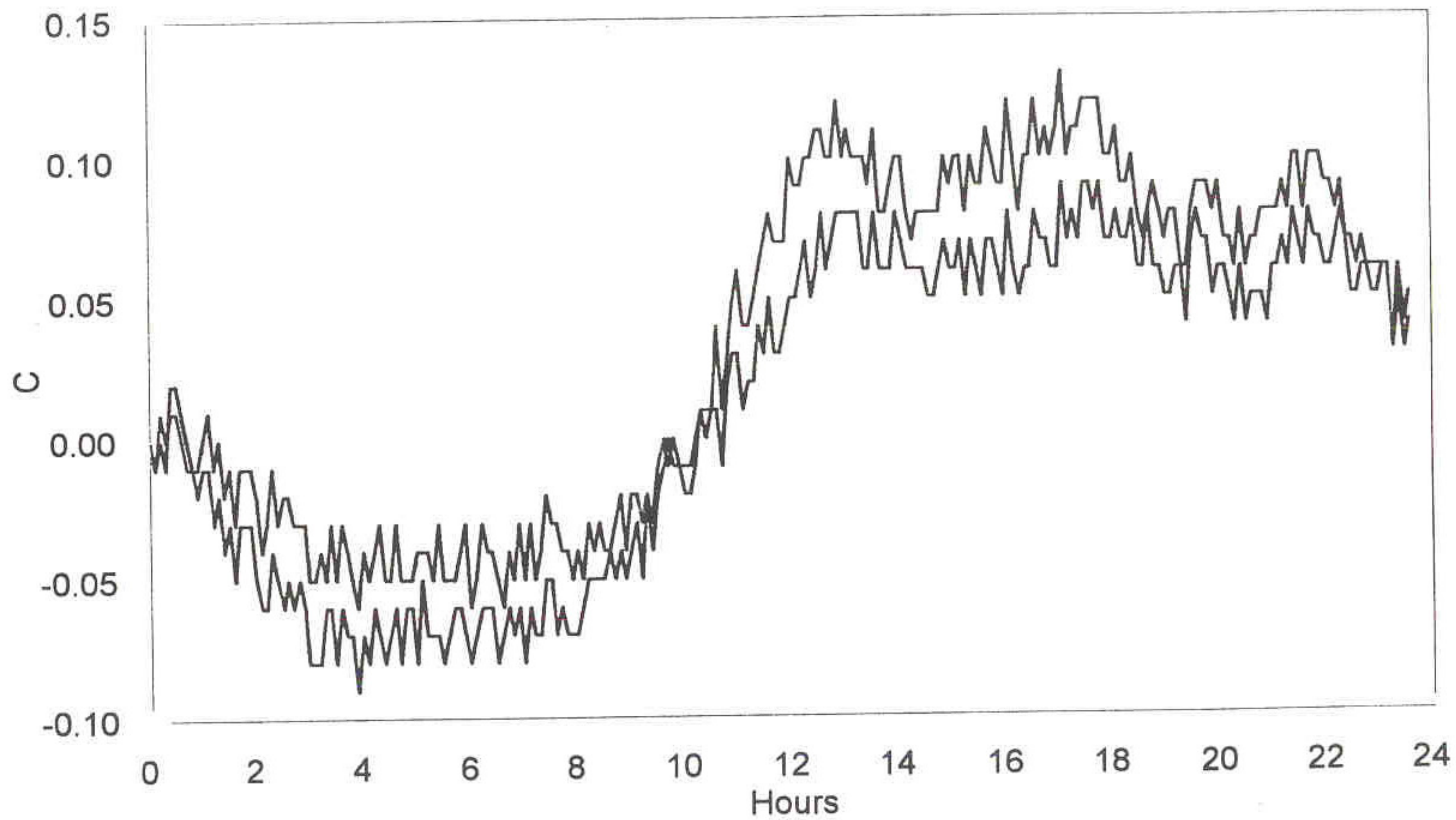


1999-07-08



Periscope 3 Temperatures

990222 1130, Delta T's



— South minus West — East minus West

Summary:

- Even though effective dispersion correction is currently limited to very bright stars, and constant-term variations are only partially controlled, solutions are sufficiently accurate to detect relatively large errors in FK5 positions relative to Hipparcos positions.
- Baselines & C-term sufficiently stable for relative astrometry over angles $\sim 10^\circ$ to < 20 mas (HR5110, relative to nearby, bright Hipparcos stars).
- Current efforts center on improving coherent averaging/dispersion correction technique & reducing constant-term drifts
 - consistent dispersion correction at the $< 1 \mu\text{m}$ level, and constant-term stability equal to that seen in lab environment should allow effective use of baseline metrology results, and should make astrometry at ~ 10 mas routine.
 - IR metrology of all (most) of feed paths may be necessary to interpolate constant-term values with sufficient accuracy for 1-3 mas astrometry.
- Developing purely IR fringe tracking capability (~ 1 yr).
 - even w/current accuracy, could significantly improve position & detect p.m. of BN object in Orion in ~ 2 yrs.

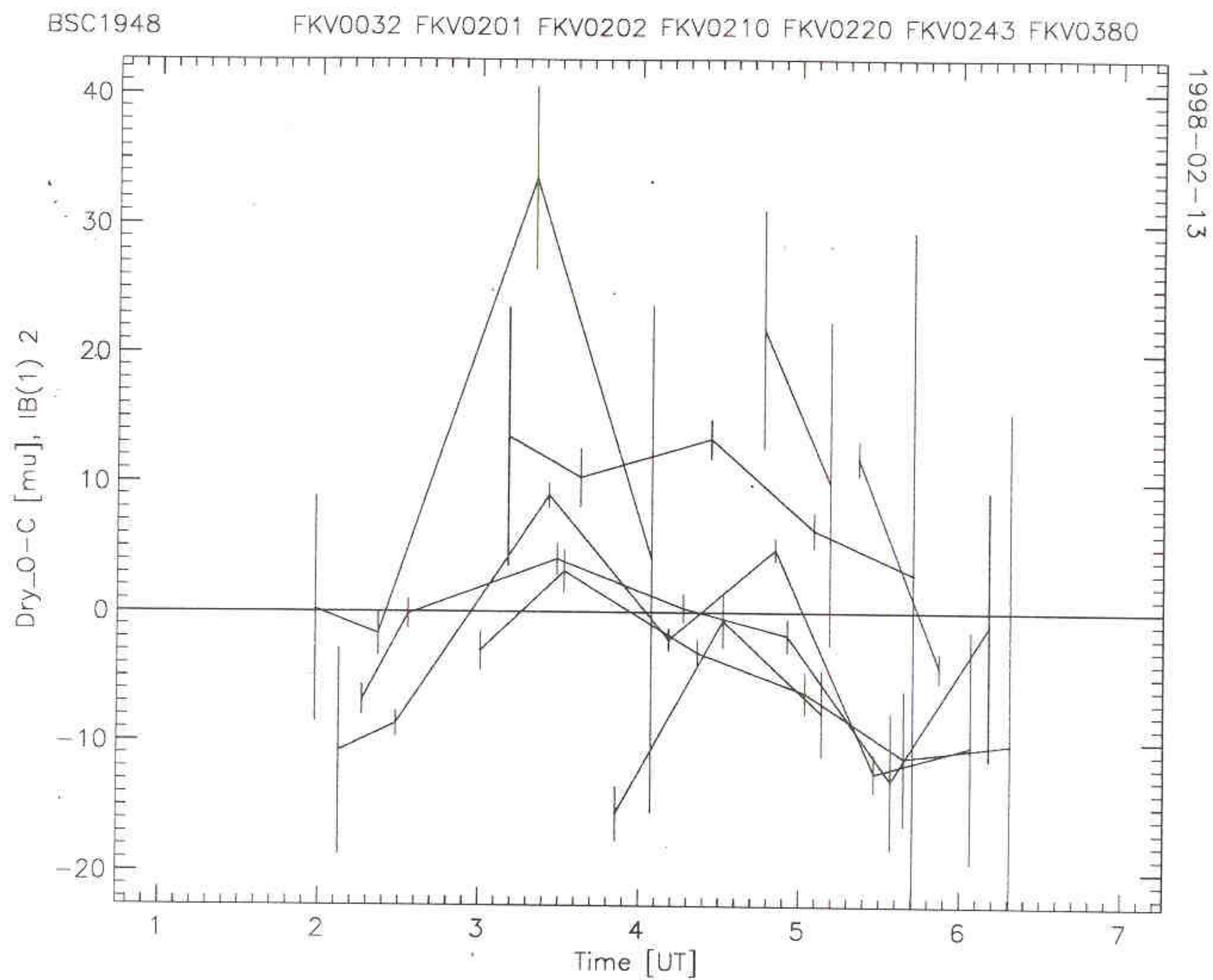


Figure 8. Data from Fig. 5, now expressed as delay residuals from a best-fit baseline computed from nominal FK5 positions of the observed stars, rather than Hipparcos positions, as used in Figs. 1 - 5.

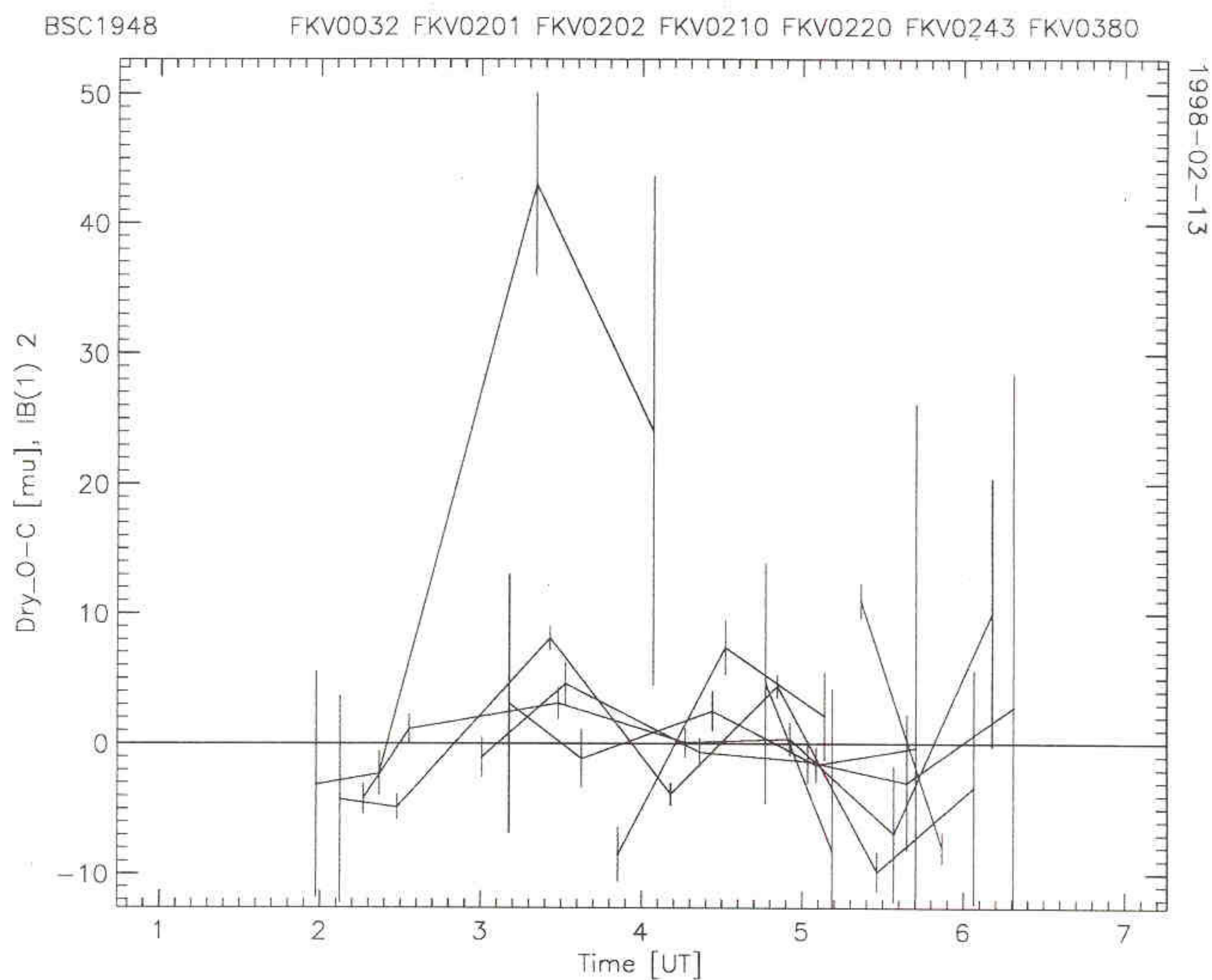


Figure 9. Residuals from the best-fit baseline in a full astrometric solution, including baseline coordinates and star position offsets (from nominal FK5 coordinates). Note the significant reduction in the residuals, relative to those in Fig. 8.

References:

Armstrong *et al.* 1998, ApJ, 496, 550.

Colavita *et al.* 1987 Appl Opt, 26, 4113.

Hines *et al.* 1990, Proc. SPIE, 1237, 87.

Hummel *et al.* 1994, ApJ, 108, 326.

Hutter *et al.* 1998, Proc. SPIE, 3350, 452.